Role of neoclassical mechanisms in the formation of a tokamak scrape-off layer

V. Rozhansky[1], E. Kaveeva[1], I. Senichenkov[1], E. Vekshina[1]
[1]*Peter the Great St.Petersburg Polytechnic University, St.Petersburg, Russia*

1. Introduction

Understanding of the mechanisms responsible for the formation of tokamak SOL is crucial for ITER as well as for future reactors. It is necessary to understand inverse dependence of the SOL width on the plasma current observed on present day tokamaks. Grad B drift could be a candidate for a mechanism of SOL formation as was suggested by Goldston [1]. However, the radial ion flux caused by grad B drift should be considered together with the radial ion $\vec{E}\times\vec{B}$ drift as it was done in the standard neoclassical theory for closed flux surfaces, and the resulting flux is determined by ion viscosity [2].

Below role of neoclassical mechanisms is analyzed. It is shown that neoclassical mechanisms can give SOL width of the order of ion Larmor radius multiplied by safety factor in accordance with the observed inverse current dependence. Radial transport is followed by radial current which is short-circuited through the divertor plates. The analytics is supported by modeling of edge plasma by SOLPS5.2 code [2] with the reduced anomalous transport coefficients in the SOL. These results are in agreement with the earlier modeling with reduced anomalous diffusion coefficient [3].

A possibility of contribution from blob (filament) transport to the SOL formation is also considered. It is shown that blob transport can also give inverse current dependence of the SOL width.

2. Neoclassical flows in the SOL

As is known from standard neoclassical theory the volume averaged radial flux of ions and electrons on the closed flux surfaces could be expressed through parallel friction and thermal force:

$$\left\langle \Gamma_{ey} \right\rangle = \left\langle \frac{1}{eB_x}\left[0.51 n m_e \nu_{ei}(u_{e\|}-u_{i\|}) + 0.71 n \frac{B_x}{B}\frac{\partial T_e}{h_x \partial x}\right]\right\rangle. \qquad (1)$$

$$\left\langle \Gamma_{iy} \right\rangle = \left\langle \frac{1}{eB_x}\left[0.51 n m_e \boldsymbol{\nu}_{ei}(u_{e\|}-u_{i\|}) + 0.71 n \frac{B_x}{B}\frac{\partial T_e}{h_x \partial x}\right] + \frac{(\nabla\cdot\vec{\vec{\boldsymbol{\pi}}}_i)_\|}{eB_x} + \frac{F^{in}}{eB_x}\right\rangle. \qquad (2)$$

Here *x* is the poloidal, *y* is radial, *z* is toroidal coordinate, h_x, h_y, h_z are metric coefficients, $(\nabla \cdot \vec{\pi}_i)_\parallel$ is parallel viscosity and F^{in} is inertia. The electron flux Eq. (1) on the closed flux surfaces is very small due to adiabatic response of electrons, the ion flux is also small and equal to the electron one provided the radial electric field is given by the neoclassical expression. Hence the neoclassical particle flux cannot be invoked to explain experimentally observed flux through the separatrix.

In contrast in the SOL parallel viscosity and inertia in Eq. (2) remain relatively large since the radial electric field in the SOL is far from the neoclassical one and has different sign. Note that this implies radial current in the SOL which should be closed through the divertor plates, see Fig.1. Assuming that Pfirsch-Schlueter parallel flows dominate in the SOL after combining parallel and toroidal momentum balance equations one obtains [2]

$$I_y = \int_{x_1}^{x_2} h_x h_z \sigma_{NEO} (E_y - E_y^{NEO}) dx \; ; \quad \sigma_{NEO} = \frac{3\mu_{i1} B}{B_x \langle B B_x \rangle} \frac{\left\langle (\frac{\vec{B}}{B} \cdot \nabla B)^2 \right\rangle}{\langle B^2 \rangle}, \tag{3}$$

where μ_{i1} is a viscosity coefficient, integration is performed above the X-point, and

$$E_y^{NEO} = \frac{T_i}{e} (\frac{1}{h_y} \frac{\partial \ln n}{\partial y} + k_T \frac{1}{h_y} \frac{d \ln T_i}{\partial y}) - \frac{B_x}{B} \langle B u_{i\parallel} \rangle . \tag{4}$$

We can estimate divergence of the net radial current (or radial flux)

$$\frac{I_y}{S L_n} \sim \frac{j_\parallel}{L_\parallel} \sim ne (\frac{\rho_{ci}}{B_x / B})^2 \frac{c_s}{q R L_n^2} \frac{c_s}{q R \nu_{ii}} \varepsilon^2 . \tag{5}$$

Here $S = \int_{x_1}^{x_2} h_x h_z dx$, $\varepsilon = r / R$, $c_s = \sqrt{(T_e + T_i)/m_i}$ is the sound speed, ρ_{ci} is the ion gyroradius. Estimating the parallel ion flow closing the radial current as nc_s and parallel current as $j_\parallel = enc_s$, for the density fall-off length we obtain

$$L_n \sim q \rho_{ci} (\frac{c_s}{q R \nu_{ii}})^{1/2} . \tag{6}$$

Estimate for the density fall-off length differs from the estimate of [1] by a factor $(\frac{c_s}{q R \nu_{ii}})^{1/2}$ which in the fluid case is smaller than unity. The reason for this difference is connected with the fact that the radial ∇B drift of ions is partially self-compensated at the flux surface. However, practically the factor $\frac{c_s}{q R \nu_{ii}}$ is smaller but not far from unity and the estimate of [1]

$L_n \sim q\rho_{ci}$ seems to be reasonable. Neoclassical estimate for electron temperature fall-off length can be done similarly [2], $L_T \le L_n$.

3. Numerical modeling of the classical SOL

Results of simulations with reduced turbulent transport coefficients in the SOL are shown in Fig.2a The simulation of H-mode shot #34439 of the Globus-M tokamak with large turbulent transport coefficients is used as a reference case. One can see that indeed after reduction of the electron heat conductivity by a factor 10, and particle diffusivity by 2, the density and temperature fall-off remain finite due to neoclassical transport in the SOL. The rise of radial current in the SOL as well as currents to the plates is clearly seen in Fig.3.

4. Blobby transport as a possible candidate for temperature fall-off

Below presented are estimates for electron temperature fall–off length under the assumption that it is determined by blobby radial electron heat transport. The blob velocity attached to the target is [4]-[5].

$$V_B = \frac{2T_e^t(T_e+T_i)\delta nq}{e^2B^2l_\perp^2 n_t c_s^t}. \qquad (7)$$

Note that radial velocity of individual blob with a given scale $l_\perp$ and density perturbation is inversely proportional to the plasma current as is observed in the experiments [6]. The SOL width can be estimated as electron temperature fall-off length from the condition

$$l_T = V_B\tau = V_B\frac{L_\parallel^2}{\chi_{e\parallel}} = V_B\frac{k^2q^2R^2}{\chi_{e\parallel}}. \qquad (8)$$

Here $L_\parallel = kqR$ with k being numerical coefficient. We assume that the spectrum of the turbulence is determined by the strong turbulence estimate $\delta n/l_\perp \sim n/l_T$ and contribution from different scales to the radial flux is of the same order $\delta nV_B \sim nV_B(n)$, where $V_B(n)$ is the velocity of perturbations with $l_\perp = l_T$ and $\delta n = n$. For l_T one obtains

$$l_T = \alpha^{1/3}\left(\frac{\rho_{ci}^2}{R}\frac{\nu_e}{c_s}\frac{m_e}{m_i}\right)^{1/3}qR, \qquad \alpha = \frac{2k^2}{3.16}\frac{nc_s}{n_t c_s^t},\ c_s = \sqrt{\frac{T_e+T_i}{m_i}}. \qquad (9)$$

The work is done in the Peter the Great Saint Petersburg Polytechnic University under support of the Russian Scientific Foundation, Grant No. 17-12-01020.

References

[1] Goldston R J 2012 *Nucl. Fusion* **52** 013009

[2] Rozhansky V, Kaveeva E, Senichenkov I, Vekshina E 2018 *Plasma Phys. Control. Fusion* **60** 035001

[3] Meier E T, Goldston R J, Kaveeva E G, Makowski M A, Mordijck S, RozhanskyV A, Senichenkov I Yu, Voskoboynikov S P 2016 *Plasma Phys. Control. Fusion* **58** 125012

[4] Krasheninnikov S I 2001 *Phys. Lett.* A **283** 368

[5] Rozhansky V and Kirk A 2008 *Plasma Phys. Control. Fusion* **50** 025008

[6] Kirk A et al 2016 *Plasma Phys. Control. Fusion* **58** 085008

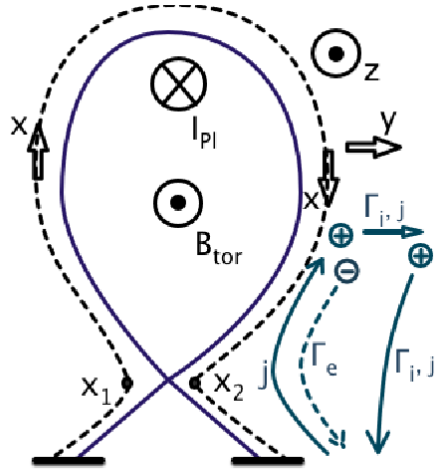

Fig. 1. General geometry and particle flows in the SOL

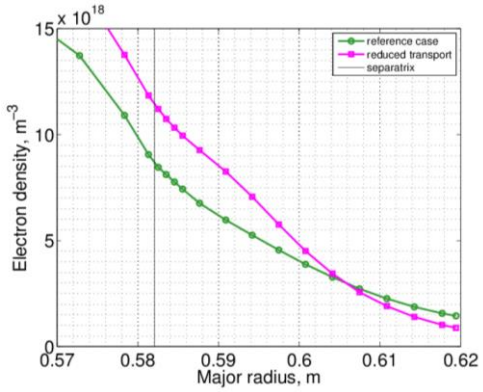

Fig. 2a. Electron density at the outer midplane

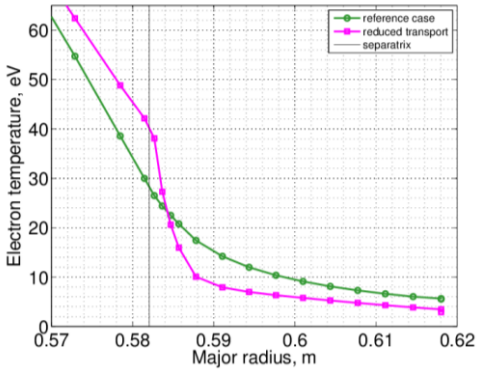

Fig. 2b Electron temperature at the outer midplane

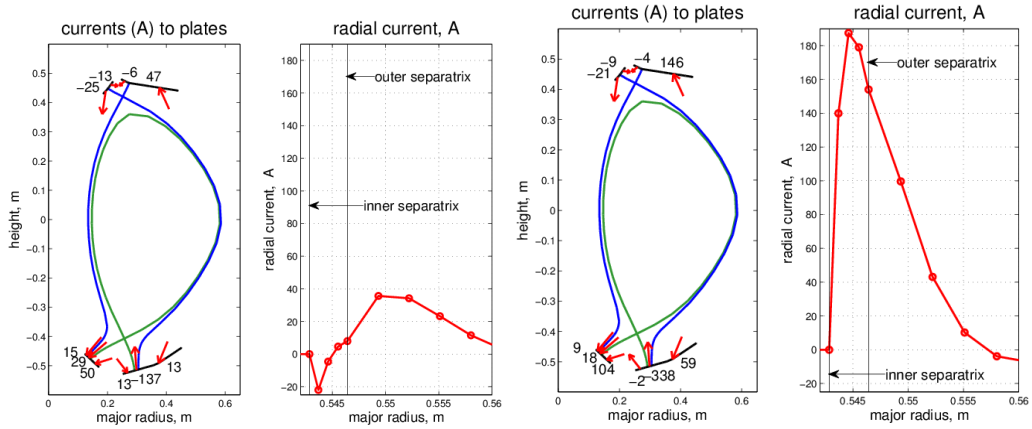

Fig. 3. Electric currents from plasma to four divertor targets are shown on left plots. Positive value stands for the current directed from plasma to the target. Upper targets are divided in two parts - private flux region and SOL. Lower targets are divided in three parts - between private flux region and outer SOL is the region connecting inner and outer lower divertor plates. Radial current integrated along the open flux surfaces in the SOL (with exception of divertor regions) is plotted on right plots. (a) reference modeling, (b) modeling with reduced transport coefficients.